

Three-dimensional reconstruction of plants and a single building from UAV images

Yu Ma^{1,2#}, Yinwen Chen^{3#}, Lifeng Zhang¹, Zhitao Zhang^{2*}, Jiarui Wang², Weihua Yu²,
Zheng Xing², Yaohua Hu⁴, Zhijie Liu⁴

(1. *Water Resources Center, Yellow River Conservancy Commission of the Ministry of Water Resources, Zhengzhou 450000, China;*

2. *College of Water Resources and Architectural Engineering, Northwest A&F University, Yangling 712100, China;*

3. *Department of Foreign Languages, Northwest A&F University, Yangling 712100, China;*

4. *College of Mechanical and Electronic Engineering, Northwest A&F University, Yangling 712100, China)*

Abstract: The three-dimensional (3D) models of buildings and plants from UAV images become increasingly popular for city construction. However, whether the previous 3D modeling precision of large-scale buildings can be further enhanced and whether that of plants from UAV images is acceptable still remain to be investigated. For these ends, this research studied the 3D modeling precision of a basketball hall and a row of *Euonymus japonicas* based on images from a DJI Inspire-1 UAV system. The data were processed with Pix4D to calculate the camera parameters, which were then processed with ContextCapture and Photoscan to generate the 3D models. The displayed height, width and crown breadth in the 3D models with the actual measured data were compared. The results showed that the errors of the 3D models in each method were within tolerance. The ContextCapture displayed a higher accuracy while the Photoscan a higher reconstruction efficiency. The r.m.s. of the respective percentage errors for the basketball hall with Photoscan and ContextCapture were 4.9 cm and 2.3 cm while those for the *Euonymus japonicas* were 1.2 cm and 0.7 cm. The results reveal two implications: the large-scale modeling precision in theory can be improved; the plants modeling from UAV images can be a better alternative because of its satisfying precision as well as its own much lower cost and less redundant data.

Keywords: UAV photogrammetry, 3D reconstruction, precision, single building, plants

DOI: 10.33440/ijpaa.20200304.141

Citation: Ma Y, Chen Y W, Zhang L F, Zhang Z T, Wang J R, Yu W H, Xing Z, Hu Y H, Liu Z J. Three-dimensional reconstruction of plants and a single building from UAV images. *Int J Precis Agric Aviat*, 2020; 3(4): 80–88.

1 Introduction

There has been a growing interest in accurate 3D modeling of varied objects in diverse engineering over the past decade. 3D models are mainly generated using 3D reconstruction, which studies how to acquire 3D information of the objects in space through its 2D information^[1].

So far 3D reconstruction can be accomplished by either active or passive methods. In particular, the image-based passive method has made significant progress with the development of

computer vision technique^[2]. Idesawa^[3] first raised the issue of recovering the 3D structure from 2D images, interpreted the principle of 3D reconstruction with mathematical method, and calculated values of space point and lines to determine their positions in the space. His study has significant influence on the subsequent researches on 3D reconstruction. Since then, 3D modeling has been extensively applied in various fields of engineering such as post-earthquake visualization management^[4], dynamic monitoring of coastline^[5,6], geologic and gully structural modeling^[7-10], and three-dimensional green biomass^[11]. With the development of urban construction, urban planning increasingly relies on 3D modeling. Google Earth and Bing Maps are the earliest interactive visualization of 3D city models open to the general public^[12]. Such visualizations are applicable to models of relatively coarse buildings at medium and large scale, and are usually limited to roof structures and planar facades.

The quality and acquisition efficiency of the raw data are fundamental to 3D modeling, so different technology has been used to obtain raw data of various objects. LiDAR technology, with continuously increasing density and accuracy of point clouds, can generate 3D point clouds and 2.5D raster at a high accuracy but produce the redundant data and extremely high cost^[13]. Compared with LiDAR technology, satellite remote sensing, with less redundant data and lower cost, can improve the reconstruction efficiency, but its data are more difficult to obtain, and lower in spatial resolution^[8,14]. Besides, a hand-held or digital camera, though with a much lower cost, higher image resolution and higher modeling precision, is limited to the image acquisition of such small objects as cars and flowers at low altitude^[15-18].

Received date: 2020-10-19 **Accepted date:** 2020-12-10

Biographies: **Yu Ma**, Assistant Engineer, research interest: Application of remote sensing technology in 3D reconstruction and water resources, Email: m1968970824@163.com; **Yinwen Chen**, lecturer, research interests: academic writing and publishing, ESP, Email: martinchen@nwfau.edu.cn; **Lifeng Zhang**, Senior Economist, research interest: economy in water resources, Email: zlf1688@sina.com; **Jiarui Wang**, Assistant Engineer, research interest: Application of remote sensing technology in 3D reconstruction Email: 2017051957@nwfau.edu.cn; **Weihua Yu**, PhD, lecturer, research interest: Application of surveying and mapping in water resources; Email: yuweihua@nwsuaf.edu.cn; **Zheng Xing**, Master student, research interest: Application of remote sensing technology in water-saving irrigation and water resources; Email: yizhi199708@163.com; **Yaohua Hu**, PhD, Professor, research interest: Integrated application of agriculture and machinery; Email: huyaohua@nwsuaf.edu.cn; **Zhijie Liu**, lecture, research interest: Integrated application of agriculture and machinery, Email: liuzhijie@nwsuaf.edu.cn.

* **Corresponding author: Zhitao Zhang**, PhD, Associate Professor, research interest: Application of remote sensing technology in water-saving irrigation and water resources. Mailing address: Northwest A&F University, Xingong Road, Yangling District, Xianyang City, 712100, China. Email: zhitaozhang@126.com.

These authors contributed equally to this research.

With the popularization of Unmanned Aerial Vehicle (UAV) technology, people began to acquire images from UAV with such advantages as low cost, simple operation, and relatively high resolution. Many researchers^[19-21] obtained images from UAV at a high flight altitude, which could reach the accuracy for usual cartographic mapping and urban-scale analysis. Xie F F^[22] utilized a parametric method, based on the images from UAV carrying four combined cameras, to reconstruct 3D models of buildings at a large scale. This method can meet the accuracy requirement of the mapping scales of 1:1000 and 1:500, but the data processors need to be highly skilled. Some researchers^[23,24] used commercial or open-source software to process the data acquired by UAV oblique photogrammetry. This photogrammetry can ensure that the data contain such details as the facades and footprints of buildings. In addition, 3D model reconstruction using the software is easy and the accuracy can be guaranteed. However, we questioned whether the precision of large-scale 3D modeling could be improved, so we compared the 3D modeling precision of a single building with large-scale ones. If the precision of the former is higher than that of the latter, we can in theory improve the precision of large-scale 3D modeling, and thus explore the corresponding method.

Chéné et al.^[25] constructed 3D canopy models of a variety of plants based on the canopy depth images captured by a low-cost depth camera with a low resolution and small scanning range. Raunonen et al.^[26] designed a rapid automatic 3D modeling method for tree canopy based on laser scanner, which can quickly obtain the point cloud data from different angles. Grocholsky^[27] installed the laser line scanner behind the test vehicle, and obtained the 3D model map of the grape vines. However, both laser scanner and vehicle-mounted or airborne radar have the following disadvantages: the original data obtained are too large in amount; and the point cloud has to be desiccated and registered first. The FASTSCAN laser scanner, developed by an American company Polhemus, can obtain the complete 3D point clouds of the plant in a single scan without point cloud registration. However, it has high environment requirements such as no metal objects around, and no outdoor application^[28]. Many researchers used 3D digitizers, which can obtain 3D morphological structure model with high precision, to reconstruct 3D models of maize^[29], rice^[30], apple tree^[31,32] and tomatoes^[33], but the measurement is time-consuming. Therefore, it is infeasible to simply use the 3D digitizer for 3D reconstruction of plants at a large scale. With the application of UAV in 3D buildings modeling, researchers used the UAV images to build plant models mainly to acquire the stand factors such as crown diameter^[34,35], tree height^[35,36] or the biomass^[37-39].

Compared with the satellite remote sensing, UAV can work at a required altitude under the cloud so that the image resolution can be improved. Meanwhile, different from the traditional aerial survey, UAVs can reduce training cost in a project and safety risks for operators through ground remote control. UAV can also overcome hand-held cameras' defects of either image acquisition of objects only at a small scale or the extremely heavy workload of image obtaining at large scale.

Buildings and plants are two essential components in urban planning. In theory, scale is not a determinant of 3D modeling accuracy, so in order to save research cost, we used the UAV to obtain images of a single building (a basketball hall) and a row of plants (*Euonymus japonicas*). Based on the acquired images, we reconstructed 3D models, and compared the distance measured on the 3D models with that of the basketball hall measured with a total

station and the *Euonymus japonicas* with the tapeline. In so doing, we mainly aim to: (1) analyze a single building 3D model precision so as to confirm whether the large-scale modeling precision can be further improved; and (2) explore the 3D modeling effects of plants based on UAV images.

2 Materials and methods

2.1 Research Objects

The basketball hall is a single architecture with no buildings around but two tall trees at the south side of it, which may influence the reconstruction effect of this part. The basketball hall is about 15 m high and 55 m width. The trees beside are little taller than the basketball hall and about 3 m from it. The *Euonymus japonicus* are in a row, next to the *Euonymus japonicus* are a row of apricot trees and there are many leaves fallen on the ground. For these two experiments, despite some influencing factors, the UAV flight could be carried out normally, and the operators were cautious enough not to crash with the obstacles.

2.2 Data acquisition

2.2.1 The UAV System

In this study, the DJI Inspire-1 UAV system was used to capture the images. The system (Figure 1) consists of a camera (Figure 1a), a UAV (Figure 1b), and a remote control with iPad (Figure 1c). The camera is a ZenmuseX3 with a resolution of 4000×3000 pixel. The detailed parameters are shown below.



Figure 1 The UAV system

Table 1 The parameters of UAV systems

DJI Inspire-1 UAV	
Parameters	Value
The gross machine weight	3.06 kg
Wheelbase	559 mm
Duration of flight	18 min
Maximum tolerable wind speed	10 m/s
Maximum pitch angle	35°
Maximum horizontal flight speed	79 km/h
The rotation range of cradle head	Horizontal: ±320° Vertical: -90°~ +30°
GPS hover precision	Horizontal: ±0.5 m Vertical: ±2.5 m

Table 2 The parameters of Camera

Zenmuse-X3 Camera	
Parameters	Value
Maximum resolution	4000×3000 pixel
Range of ISO	Photo: 100~1600 Video: 100~3200
Sensor type	1/2.3" CMOS
Sensor Dimensions	6.170 (mm)×4.628 (mm)
Focal length	2302.347 pixel
Pixel size	1.58 μm

2.2.2 Data Collection of the Basketball Hall

The experiment of the basketball hall was carried out in the north campus of Northwest A&F University in December, 2018. In order to obtain the maximally accurate details, we conducted the experiment with nadir and oblique flight to obtain the building facades and footprints respectively in a sunny and windless morning. For the nadir flight, we routed the UAV flight using the matching flight software DJI GO pro (The forward and side overlap was 80% and 75%, respectively.), while the oblique flight was in manual mode.

Figure 2 shows the camera position of the flight. There were not enough photos at the north side due to the tall trees there. Figure 3 shows the south side of the basketball hall and there exist two tall trees, which are real obstacles to the photography.

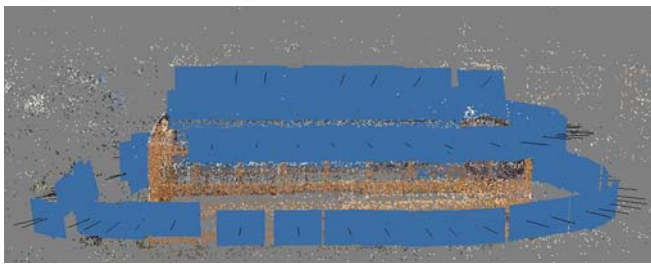


Figure 2 The position of the camera



Figure 3 The south side of the basketball hall

Apart from the UAV flight, we also need to do an experiment to obtain the actual data of the basketball hall. We set 11 key points on the basketball and used the total station to acquire the relative coordinates of them. In order to improve the accuracy of such operations when a reflective prism is unusable as landslide observation, deformation measurement, and tunnel construction. We need to acquire the height of the hall, but it is inconvenient for us to put the prism onto the top of the building, so we chose the prism-free total station.

2.2.3 Data Collection of Euonymus Japonicas

The *Euonymus japonicus* in a row were roughly of the same shape. The UAV system was the same as was used in the first experiment. In the second experiment, both nadir and oblique flights were also taken in order to guarantee the accuracy of the 3D model. Because the research area was too small, it was necessary to state that both the nadir and oblique flight were in manual mode. In the flying, we had been on alert to the surrounding environment in case the UAV be destroyed. Figure 4 shows the camera position of the flight.

Since the *Euonymus japonicus* were small in size, we used tapeline to measure the height and crown breadth (CB). The CB of each plant is the average width in the north-south and east-west directions.



Figure 4 The position of the camera

2.3 Data Processing

The images obtained by digital cameras or UAV can be utilized to generate dense point cloud of the target objects using several commercial or open-source software such as VisualSFM, Pix4D, Photoscan, PhotoModel, and ContextCapture^[23,24,40,41]. Among the software, ContextCapture can create denser cloud^[24], which in theory is the basis to construct 3D models of higher precision.

Before the data processing, the images were pre-processed with Photoscan. In the preparation, we first created a project, and then added the obtained images into the project. Next the quality index of each acquired image was calculated with the image quality assessment tool. The images, whose quality index is higher than 0.8 (the quality index is between 0 and 1), were used for model reconstruction. If the quality index of the images is lower than 0.5,

the images may have exposure and focus problems. These images that are not suitable for subsequent 3D reconstruction should be discarded. If the quality index is between 0.5 and 0.8, we can improve the image quality through color matching, and these images can be processed with images of high quality. In our experiments, the quality indexes of all images acquired from the flight were all above 0.8, so they could be used for subsequent processing. The pre-processing has verified that 70% of the overlap was guaranteed for the two experiments.

After the pre-processing, we used the Pix4D-mapper^[42,43] to calculate the accurate camera interior and exterior orientation elements^[44]. The calculated parameters are shown above in Tables 1 and 2. Based on the parameters, two software packages, Photoscan and ContextCapture, were used to generate the 3D models of the two objects.

2.3.1 Basketball Hall Image Processing with Photoscan

Photoscan^[45] is able to generate an accurate 3D model without camera calibration. The rough workflow is listed as follows: image checking and aligning, sparse and dense clouds building, and Mesh (TIN model) and texture building. Followed is the export of the DEM, ortho-mosaic, Mesh and 3D model of the study object.

During each procedure, the image processing involves the parameters which are shown in Table 3.

Table 3 The parameters in the image processing

Procedure	Parameters
Align the images	Accuracy: High (using the whole image scale) Pair preselection: Reference Other parameters are default (Key point limit:40000; Tie point limit:4000)
Build dense cloud	Quality: Medium (the initial images shrink 1/16) Depth: Moderate Reuse depth maps: No
Generate the Mesh and create TIN model	Surface type: Height field Source data: Dense cloud Face count: High (1/5 number of the point cloud) Other parameters are default: (Interpolation: Enabled)
Obtain 3D model	Mapping mode: Generic Blending mode: Mosaic(default) Texture size/count: 8000*2 (The previous size number are supposed to be less than 9000 if we need export the Adobe 3D pdf for easily view)

After this series of image processing with the set parameters, we finally obtained the 3D models of the basketball hall. Below are three views of the 3D model. As is shown in Figure 6, on the wall there are shadows of the trees on the south side of the basketball hall.



Figure 5 The front view of the basketball hall 3D model



Figure 6 The side view of the basketball hall 3D model



Figure 7 The vertical view of the basketball hall 3D model

2.3.2 Basketball Hall Image Processing with ContextCapture

ContextCapture^[46], based on GPU of graphics operation unit, can produce the real 3D model automatically from a sequence of overlapping images. The software, with four main modules can measure space distance and height difference as well as the coordinates of points.

ContextCapture can generate such different kinds of formats as OSGB, .obj, S3C, and STL. As is shown in Figure 15, the south part of the basketball hall is so obviously affected by the presence of the trees that the UAV can't take sufficient images of this part. The data inclusive of that part could be obtained in a season when the trees are leafless. Otherwise, the model has to be completed with the aid of the TLS or repaired in the Meshlab program to delete the noise.

In the image processing with ContextCapture, a block was first created to add images in, and then the aerotriangulation was submitted so as to automatically and accurately estimate the image position and camera properties (focal length, principal point, and lens distortion). With the help of Engine, the aerotriangulation operated normally with new production. Next the new production was submitted, and the S3C format was chosen for output, which could be opened with the Viewer module. In the texture compression we chose the 75% quality JPEG, which can ensure the 3D model quality and the reconstruction efficiency. The final 3D model of the basketball hall with different views is shown in Figures 8, 9, and 10.

The images of the *Euonymus japonicas* were also processed with Photoscan and ContextCapture, and the procedure was the same as that in the basketball hall image processing. The different views of the *Euonymus japonicas* 3D models generated with the two methods are shown in the following two sub-sections.



Figure 8 The front view of the basketball hall 3D model



Figure 9 The side view of the basketball hall 3D model



Figure 10 The vertical view of the basketball hall 3D model

2.3.3 Euonymus Japonicus Image Processing with Photoscan



Figure 11 The front view of the Euonymus japonicus 3D model



Figure 12 The vertical view of the Euonymus japonicus 3D model

2.3.4 Euonymus Japonicus Image Processing with ContextCapture

Judging from the different views of the basketball hall and the Euonymus japonicas obtained by the two methods, we can see that ContextCapture outperforms Photoscan in visual details. Photoscan can more easily divide areas when modeling, thus reducing unnecessary noise and modelling time.



Figure 13 The front view of the Euonymus japonicus 3D model



Figure 14 The vertical view of the Euonymus japonicus 3D model

3 Results

3.1 Quantitative Results of Basketball Hall

We built the 3D models after the data processing, and obtained some distances between several points on the models. For the basketball hall, we selected 11 feature points so that we could obtain the sizes of the basketball hall and the window (of two different sizes) frames. The 11 points are shown in Figure 15, and the sequence number of the Euonymus japonicus in Figure 16.

In order to examine the 3D model precision of a single building, we compared 10 distances measured via total station with those measured on the 3D models. The descriptive statistics of

the comparison is shown in Table 4: SD is distance measured via total station; PD is the distance measured on the Photoscan 3D model; PE is the error between PD and SD; PPE is the absolute percentage error of the PE; CCD is the distance measured on the ContextCapture 3D model; CCE is the error between CCD and SD; and CCPE is the absolute percentage error of the CCE.



Figure 15 The feature point labels at the basketball hall



Figure 16 The sequence number of the Euonymus japonicas

Table 4 Descriptive statistics of the basketball hall distance measurements

Project	Distances	SD/m	PD /m	PE /m	PPE /%	CCD /m	CCE /m	CCPE /%
1	1-2	14.009	14.01	0.001	0.007	14	-0.009	0.064
2	2-3	54.559	54.6	0.041	0.076	54.562	0.003	0.006
3	1-11	33.901	33.86	-0.041	0.120	33.9	-0.001	0.002
4	2-9	11.064	11.08	0.016	0.142	11.072	0.008	0.070
5	9-10	12.057	12.03	-0.027	0.226	12.06	0.003	0.023
6	4-5	3.449	3.42	-0.029	0.841	3.446	-0.003	0.087
7	4-6	5.320	5.29	-0.030	0.558	5.327	0.007	0.137
8	1-4	0.635	0.637	0.002	0.384	0.638	0.003	0.542
9	7-8	3.658	3.63	-0.028	0.767	3.662	0.004	0.108
10	1-3	56.331	55.8	-0.131	0.943	56.554	0.072	0.395
		Mean (m)		-0.023			0.009	
		r.m.s. (m)		0.049			0.023	

In the study, the errors were calculated first, and then such indexes as the mean difference, root mean square (r.m.s.), and variance were used to evaluate the errors.

Table 4 shows that each of the measured distances falls within the tolerance of the cartography (column 5 and column 8). The mean PE and CCE were -2.3 cm and 0.9 cm, respectively, and such results are satisfying in cartography. The comparison between the

distances obtained from Photoscan and ContextCapture proved that the results of the latter (with an r.m.s. of 2.3 cm) outperformed the former (with an r.m.s. of 4.9 cm).

Figure 17 is a histogram more directly showing the comparison between the distances measured in different ways. As is shown in the figure, most of the measured distances display no significant difference. The fifth project shows that both PD and CCD are significantly different from the SD; in the tenth project, the CCD is much smaller than the PD.

Figure 18 is the percentage error comparison of the two 3D models. It is apparent that almost all the PPE is much larger than CCPE. In addition, it is also important to notice that both the maximum and the minimum PPEs (0.943 and 0.007, respectively) are larger than the CCPEs (0.542 and 0.002, respectively). The mean PPE and CCPE were 0.4060 and 0.1434, respectively; and the variances of the PPE and CCPE were 0.12039 and 0.03241, respectively.

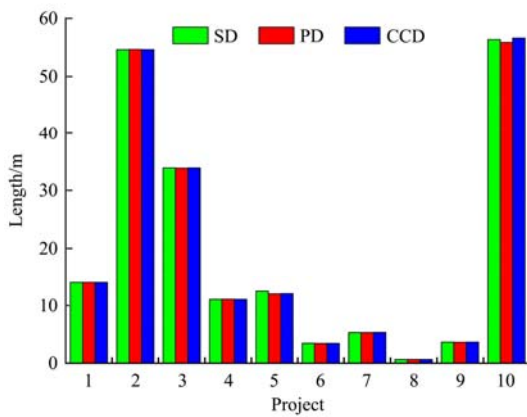


Figure 17 Histogram of the distance measurements comparison of the basketball hall

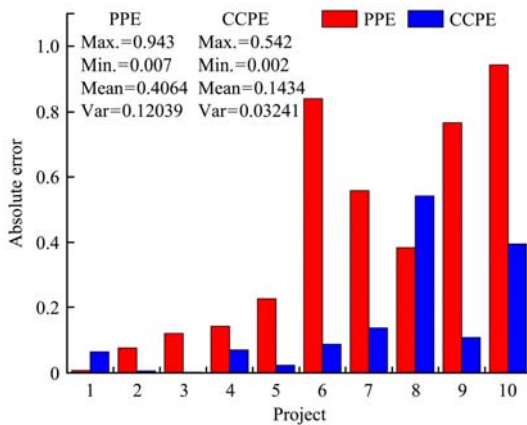


Figure 18 Percentage Error comparison of the basketball hall

3.2 Quantitative Results of Euonymus Japonicus

In order to examine the 3D model precision of a row of plants, we compared 6 distances measured via tapeline with those measured on the 3D models. The descriptive statistics of the comparison is shown in Table 5: SD is distance measured via total station; PD is the distance measured on the Photoscan 3D model; PE is the error between PD and SD; PPE is the absolute percentage error of the PE; CCD is the distance measured on the ContextCapture 3D model; CCE is the error between CCD and SD; and CCPE is the absolute percentage error of the CCE.

In Table 5, columns 4 and 7 show that the mean PE and CCE are -0.6 cm and 0.6 cm, respectively, and the r.m.s. of the two are 1.2 cm and 0.7 cm, respectively.

Table 5 Descriptive statistics of the Euonymus japonicas distance measurements

Project	Names	SD /m	PD /m	PE /m	PPE /%	CCD /m	CCE /m	CCPE /%
1	1-Height	1.585	1.570	-0.015	0.946	1.59	0.005	0.315
2	1-CB	1.425	1.43	0.005	0.351	1.43	0.005	0.351
3	2-Height	1.708	1.72	0.012	0.703	1.715	0.007	0.410
4	2-CB	1.540	1.525	-0.015	0.974	1.550	0.010	0.649
5	3-Height	1.585	1.575	-0.010	0.631	1.592	0.007	0.442
6	3-CB	1.485	1.475	-0.010	0.673	1.488	0.003	0.202
				Mean (m)	-0.006			0.006
				r.m.s.(m)	0.012			0.007

Figure 19 is a histogram more directly showing the comparison between the distances measured with different methods. As is shown in the figure, most of the measured distances are significantly different and all the six projects show that CCEs are significantly smaller than the PEs, and the results verified that ContextCapture outperformed Photoscan.

Figure 20 shows the percentage error comparison of the two 3D models, which apparently shows that the PPE is much larger than CCPE. This further confirms that ContextCapture outperforms Photoscan in precision. Similar to the result of the basketball hall, both the maximum and the minimum PPEs (0.98361 and 0.34965, respectively) were larger than the CCPEs (0.64516 and 0.20161, respectively); the mean PPE and CCPE were 0.71654 and 0.39313, respectively; and the variance of the PPE and CCPE were 0.0543 and 0.02213, respectively.

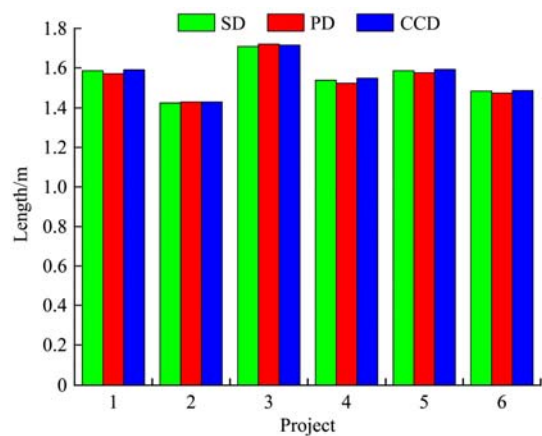


Figure 19 Histogram of the distance measurements comparison of the Euonymus japonicas

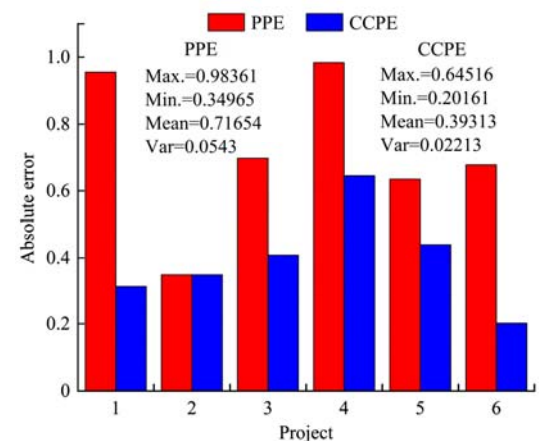


Figure 20 Percentage Error comparison of the Euonymus japonicas

4 Discussion

This study aimed to determine whether the large-scale modeling precision could be improved, and whether the plants images acquired with UAV and processed with the commercial software could be a better alternative.

We first acquired images of a single building, the basketball hall with the UAV nadir and oblique flight. After the data processing with Photoscan, we compared the 3D model measurements with the distances measured with the total station. The basketball hall 3D model results indicated that the mean error was 2.3 cm and the r.m.s. was 4.9 cm. Giuseppina Vacca^[47] obtained images from both nadir and oblique flights over an area of 3.5 hectares with 30 buildings. Then he compared the 3D model based on the data processed via Photoscan with that from the Terrestrial Laser Scanner survey, and discovered the mean error was 3 cm, and the error's r.m.s. was 6 cm, which were within the tolerance for large-scale cartography. With the same data acquiring (UAV) and processing (Photoscan) method, we found that the precision had no significant improvement in the single building 3D modeling. Then we used ContextCapture to reconstruct the basketball hall, and found it outperformed Photoscan in the 3D model accuracy, with the mean error of 0.9 cm and the r.m.s. of 2.3 cm. We can theoretically speculate that the large-scale modeling precision can be improved when ContextCapture is used for data processing.

In the second experiment, we conducted an oblique flight over a row of *Euonymus japonicus*. After data processing using the same two methods as in the first experiment, we compared the 3D model measurement of the CB and the height of the plants with the data measured with the tapeline. According to the *Euonymus japonicus* 3D model results, the error of it ranged from 0.5 cm to 1.5 cm, the mean error was 0.6 cm and the r.m.s. was 1.2 cm. These results suggest that the 3D model precision of the plants is better than that of the building using Photoscan. Subsequently, we processed the images of the *Euonymus japonicus* with ContextCapture, and found the error ranged from 0.3 cm to 1 cm, the mean error was 0.6 cm and the r.m.s. was 0.7 cm. This result also indicates ContextCapture outperforms Photoscan. Laser scanner can obtain a more accurate 3D surface with the spatial structure information but no color and texture details. Besides, the 3D scanner has higher environment requirements such as no metal objects around^[28]. Compared with the scanner, UAV can acquire images without such environment requirement. With the commercial software, the color and texture details of the plant can be satisfyingly reconstructed.

We can conclude that there is no necessary correlation between the point density and the number of the images because the basketball hall has more images but lower point density than the *Euonymus japonicus*. However, the numbers of density point cloud, model face and vertical are positively correlated with the image number. In addition, the matching and calibration of basketball hall image is longer than that of *Euonymus japonicus*. This is because the algorithm is the same, but the image matching and calibration occurs between two or three images, and that means the more images there are, the longer it takes. On the contrary, the rebuilding and UV mapping of basketball hall took less time than *Euonymus japonicus*. This probably because the texture of the *Euonymus japonicus* is much rougher than that of the basketball hall, so it will be more complicated to be recognized.

A notable result is that there is a correlation between the 3D

model accuracy and point density. During the research, we found out that *Euonymus japonicus* has apparently higher point density than the basketball hall. Tables 4 and 5 indicate the PE and r.m.s. of the *Euonymus japonicus* are both obviously smaller than those of the basketball hall. The highest accuracy is associated with the largest point number and the lowest accuracy is associated with the smallest point number. It can be assumed that the attainable accuracy relies on the point density.

5 Conclusions

In this research, we studied the 3D reconstruction effects of a basketball hall and a row of *Euonymus japonicus* with Photoscan and ContextCapture. To acquire their respective images, we conducted nadir and oblique flight over the building while an oblique flight over the plants. Next, we measured the distances on the 3D models of the two objects, and compared the measurements with the data measured by total station and tapeline, respectively.

In 3D reconstruction from UAV images, the combination of oblique and nadir flights helps to acquire the facade and the footprints of the buildings. Besides, the flying method is totally non-invasive, since the UAV can collect data from remote areas without any contact with the objects, and the method can also be adopted in an emergency situation^[48].

From the analysis of the PE, CCE, PPE, and CCPE, and the comparison with the previous studies, we concluded that: (1) compared with Photoscan, ContextCapture can be used to further improve the large-scale modeling precision; (2) compared with the traditional method, reconstructing 3D models of plants like 3D digitizers can obtain 3D morphological structure model, but the measurement is time-consuming; laser scanner can obtain the complete 3D point clouds of the plants quickly, but the environment requirements is so high. Therefore, the plants modeling from UAV images can be a better alternative to the images from the traditional technology because 3D models from UAV images have displayed satisfying precision and UAV has much lower cost and less redundant data.

Besides, we also speculated that 3D reconstruction of buildings might be quicker than plants if the numbers of the images are equal. Further studies can be carried out on the buildings and plants through acquiring the same image numbers. We can reconstruct their respective 3D models and compare the processing time to verify our speculation in later studies.

Author Contributions

Yu Ma: experiment design and conducting, data collection and analysis, paper draft and revision;

Yinwen Chen: research design, paper draft and revision;

Lifeng Zhang: research, data analysis;

Zhitao Zhang: research conception and design, final draft approval;

Weihua Yu: materials contribution;

Jiarui Wang and Zheng Xing: experiment conducting and data collection.

Yaohua Hu and Zhijie Liu: data collection

Acknowledgment

The research is supported by the National Key Research and Development Program of China (2016YFD0200700), and the Translation Program of Materials on Agricultural Science and Culture (G202008-02).

Conflicts of Interest

The authors declare there is no conflict of interest.

[References]

- [1] Sheyan, J. 3D Reconstruction Based on Image Sequence. 2006; Master thesis, Jilin University, Changchun.
- [2] Remondino, F, Hakim S E. Image-based 3D Modelling: A Review. *The Photogrammetric Record*, 2006; 21, 269–291. doi: 10.1111/j.1477-9730.2006.00383.x
- [3] Idesawa M.. A System to Generate a Solid Figure from Three View. *Bulletin of the JSME*, 1973; 16, 216–225. doi: 10.1299/kikai1938.38.1267
- [4] Zhou J P, Gong J H, Wang T et al. Study on UAV Remote Sensing Image Acquiring and Visualization Management System for the Area Affected by 5.12 Wenchuan Earthquake. *Journal of Remote Sensing*, 2008; 06, 877–884. doi: 10.3321/j.issn:1007-4619.2008.06.009
- [5] Harwin S, Lucieer A. Assessing the Accuracy of Georeferenced Point Clouds Produced via Multi-View Stereopsis from Unmanned Aerial Vehicle (UAV) Imagery. *Remote Sensing*, 2012; 4, 1573–1599. doi: 10.3390/rs4061573
- [6] Li H, Yu Z d, Cai X b et al. River Terrace Extraction Based on Unmanned Aerial Vehicle Remote Sensing. *Earth Science*, 2017; 05, 734–742. doi: 10.3799/dqkx.2017.061
- [7] Svennevig, K, Guarnieri P, Stemmerik L. From oblique photogrammetry to a 3D model Structural modeling of Kilen, eastern North Greenland. *Computers & Geosciences*, 2015; 83, 120–126. doi: 10.1016/j.cageo.2015.07.008
- [8] Kristen L, Cook. An evaluation of the effectiveness of low-cost UAVs and structure from motion for geomorphic change detection. *Geomorphology*, 2017; 278, 195–208. doi: 10.1016/j.geomorph.2016.11.009
- [9] Rossi P, Mancini F, Dubbini M et al. Combining nadir and oblique UAV imagery to reconstruct quarry topography: methodology and feasibility analysis. *European Journal of Remote Sensing*, 2017; 50, 211–221. doi: 10.1080/22797254.2017.1313097
- [10] Mali V K, Kuiry S N. Assessing the accuracy of high-resolution topographic data generated using freely available packages based on SfM-MVS approach. *Measurement*, 2018; 124, 338–350. doi: 10.1016/j.measurement.2018.04.043
- [11] Liang H l, Li W z, Zhang Q p et al. Using unmanned aerial vehicle data to assess the three-dimension green quantity of urban green space: A case study in Shanghai, China. *Landscape and Urban Planning*, 2017; 164, 81–90. doi: 10.1016/j.landurbplan.2017.04.006
- [12] Leberl F, Kluckner S, Bischof H. Collection, processing and augmentation of VR, 2009.
- [13] Haala N, Kada M. An update on automatic 3D building reconstruction. *ISPRS Journal of Photogrammetry and Remote Sensing*, 2010; 65, 570–580. doi: 10.1016/j.isprsjprs.2010.09.006
- [14] Chen J Y, Chen S B, Zhang Z T et al. Investigation on Photosynthetic Parameters of Cotton during Budding Period by Multi-spectral Remote Sensing of Unmanned Aerial Vehicle. *Transactions of the Chinese Society for Agricultural Machinery*, 2018; 10, 230–239. doi: 10.6041/j.issn.1000-1298.2018.10.026
- [15] Pollefeys M, Van G L, Maarten V et al. Visual Modeling with a Hand-Held Camera. *International Journal of Computer Vision*, 2004; 59, 207–232. doi: 10.1023/b:visi.0000025798.50602.3a
- [16] Pollefeys M, Nistér D, Frahm J M et al. Detailed Real-Time Urban 3D Reconstruction from Video. *International Journal of Computer Vision*, 2008; 78, 143–167. doi: 10.1007/s11263-007-0086-4
- [17] Zheng S y, Zhou Y. High Quality Texture Reconstruction for Small Objects Based on Structure Light Scanning System with Digital Camera. *Geomatics and Information Science of Wuhan University*, 2012; 37, 529–533. doi: 10.13203/j.whugis2012.05.002
- [18] Wierzbicki, D, Nienaltowski M. Accuracy Analysis of a 3D Model of Excavation, Created from Images Acquired with an Action Camera from Low Altitudes. *ISPRS International Journal of Geo-Information*, 2019; 8, 83. doi: 10.3390/ijgi8020083
- [19] Liu K, Dong X Y, Qiu B J. Analysis of cotton height spatial variability based on UAV-LiDAR. *Int J Precis Agric Aviat*, 2020; 3(3): 72–76. doi: 10.33440/j.ijpaa.20200303.79
- [20] Jinbao Hong, Yubin Lan, Xuejun Yue, Zhenzhao Cen, Linhui Wang, Wen Peng, Yang Lu. Adaptive target spray system based on machine vision for plant protection UAV. *Int J Precis Agric Aviat*, 2020; 3(3): 65–71. doi: 10.33440/j.ijpaa.20200303.92
- [21] Hu J, Yang J C. Application of distributed auction to multi-UAV task assignment in agriculture. *Int J Precis Agric Aviat*, 2018; 1(1): 44–50. doi: 10.33440/j.ijpaa.20180101.0008
- [22] Xie, F, Lin, Z, Gui, D et al. Study on construction of 3D building based on UAV images. *The International Archives of the Photogrammetry*, 2012; 469–473. doi: 10.5194/isprsarchives-XXXIX-B1-469-2012
- [23] Jiroušek, T, Kapica R, Vrublová D. The testing of photoscan 3D object modelling software. *Geodesy and cartography*, 2014; 40, 68–74. doi: 10.3846/20296991.2014.930251
- [24] Aicardi, I, et al. UAV PHOTOGRAMMETRY WITH OBLIQUE IMAGES: FIRST ANALYSIS ON DATA ACQUISITION AND PROCESSING. *ISPRS-International Archives of the Photogrammetry, Remote Sensing and Spatial Information Sciences*, 2016; XLI-B1, 835–842. doi: 10.5194/isprs-archives-XLI-B1-835-2016
- [25] Yann C, David R, Philippe L et al. On the use of depth camera for 3D phenotyping of entire plants. *Computers and Electronics in Agriculture*, 2012; 82, 122–127. doi: 10.1016/j.compag.2011.12.007
- [26] Raunonen P, Kaasalainen S, Kaasalainen M et al. Approximation of volume and branch size distribution of trees from laser scanner data. *International Archives of Photogrammetry, Remote Sensing and Spatial Information Sciences*, 2011; 38, 79–84. doi: 10.5194/isprsarchives-XXXVIII-5-W12-79-2011
- [27] Grocholsky B, Nuske S, Aasted M. A camera and laser system for automatic vine balance assessment. 2011 ASABE Annual International Meeting, 2012; ASABE Paper 1111651.
- [28] Fang Hui, Hu Lingchao, He R et al. Research on plant three-dimensional information acquisition method. *Transactions of the CSAE*, 2012; 28, 142–147. doi: 10.3969/j.issn.1002-6819.2012.03.025
- [29] Ma Yuntao, Guo Yan, Li Baoguo. Azimuthal distribution of maize plant leaves determined by 3D digitizer. *Acta Agronomica Sinica*, 2006; 32, 791–798. doi: 10.3321/j.issn:0496-3490.2006.06.001
- [30] Zheng Bangyou, Shi Lijuan, Ma Yuntao et al. Three-dimensional digitization in situ of rice canopies and virtual stratified clipping method. *Scientia Agricultura Sinica*, 2009; 42, 1181–1189. doi: 10.3864/j.issn.0578-1752.2009.04.008
- [31] Wang Fei, Zhang Sheqi, Li Bingzhi et al. Three-dimensional reconstruction of trees trained to tall spindle shape and assessment of light characteristics. *Northern Horticulture*, 2012; 10–13.
- [32] Zhang Lanfen. Research on digitizing in original site and fractal feature of the configuration of apple trees. 2012; Master Thesis, Northwest A&F University, Yangling.
- [33] Yuan Xiaomin, Wen Weiliang, Guo Xinyu et al. 3-Dimensional Morphology Simulation of Tomato Canopy---Based on Measured Data. *Journal of Agricultural Mechanization Research*, 2012, 172–176. doi: 10.13427/j.cnki.njyi.2012.02.052
- [34] Liu Wenping, Zhong Tingyu, Song Yining. Prediction of trees diameter at breast height based on unmanned aerial vehicle image analysis. *Transactions of the Chinese Society of Agricultural Engineering (Transactions of the CSAE)*, 2017; 33, 99–104. doi: 10.11975/j.issn.1002-6819.2017.21.012
- [35] Panagiotidis D, Abdollahnejad A, Surový Peter et al.. Determining tree height and crown diameter from high-resolution UAV imagery. *International Journal of Remote Sensing*, 2017; 38, 2392–2410. doi: 10.1080/01431161.2016.1264028
- [36] Zarco-Tejada P J, Diaz-Varela R, Angileri V et al. Tree height quantification using very high resolution imagery acquired from an unmanned aerial vehicle (UAV) and automatic 3D photo-reconstruction methods. *European Journal of Agronomy*, 2014; 55, 89–99. doi: 10.1016/j.eja.2014.01.004
- [37] Bendig J, Bolten, A, Bennertz, S et al. Estimating Biomass of Barley Using Crop Surface Models (CSMs) Derived from UAV-Based RGB Imaging. *Remote Sensing*, 2014; 6, 10395–10412 doi: 10.3390/rs61110395
- [38] Jing Ran, Gong Zhaoning, Zhao Wenji et al. Above-bottom biomass retrieval of aquatic plants with regression models and SfM data acquired by a UAV platform – A case study in Wild Duck Lake Wetland, Beijing, China. *ISPRS Journal of Photogrammetry and Remote Sensing*, 2017; 134, 122–134. doi: 10.1016/j.isprsjprs.2017.11.002
- [39] Walter James, Edwards James, McDonald Glenn et al. Photogrammetry for the estimation of wheat biomass and harvest index. *Field Crops Research*, 2018; 216, 165–174. doi: 10.1016/j.fcr.2017.11.024

- [40] Nex F C, Remondino F. UAV for 3D mapping applications: a review. *Applied geomatics*, 2014; 6, 1–15. doi: 10.1007/s12518-013-0120-x
- [41] Mousavi V, Khosravi M, Ahmadi M et al. The performance evaluation of multi-image 3D reconstruction software with different sensors. *Measurement*, 2018; 120, 1–10. doi: 10.1016/j.measurement.2018.01.058
- [42] Pix4D software. Available online: <https://pix4d.com.cn/product/pix4dmapper-pro/> (accessed on 19 November 2018)
- [43] DJI official Website. Available online: <https://www.dji.com/cn/company> (accessed on 19 November 2018)
- [44] Yu Donghai, Feng Zhongke. Tree crown volume measurement method based on oblique aerial images of UAV. *Transactions of the Chinese Society of Agricultural Engineering (Transactions of the CSAE)*, 2019; 35, 90–97. doi: 10.11975/j.issn.1002-6819.2019.01.011
- [45] Photoscan software. Available online: <http://www.agisoft.cn/> (accessed on 22 November 2018)
- [46] ContextCapture software. Available online: <http://www.cadsolutions.com.au/contextcapture/index.shtml#software> (accessed on 23 November 2018)
- [47] Vacca Giuseppina, Dessì Andrea, Sacco Alessandro. The Use of Nadir and Oblique UAV Images for Building Knowledge. *ISPRS International Journal of Geo-Information*, 2017; 6, 393. doi: 10.3390/ijgi6120393
- [48] Clark Dylan G, Ford James D, Tabish Taha. What role can unmanned aerial vehicles play in emergency response in the Arctic: A case study from Canada. *PLOS ONE*, 2018; 13, e0205299. doi: 10.1371/journal.pone.0205299